Angular dependence of the in-plane energy gap of $Bi_2Sr_2CaCu_2O_8$ by tunneling spectroscopy

Jeffrey Kane and K.-W. Ng
Department of Physics and Astronomy, University of Kentucky, Lexington, Kentucky 40506-0055
(Received 14 June 1995; revised manuscript received 29 September 1995)

A technique for tunneling into the a-b plane of the layered cuprate superconductors is described and applied to study the in-plane gap anisotropy of the high-T_c superconductor $Bi_2Sr_2CaCu_2O_8$. The results show unambiguously that the in-plane energy gap is highly anisotropic with a gap minimum along the Cu-O_2 bond direction. Using these results, we present an angular mapping of the in-plane gap anisotropy and compare our results to those from other experiments. Effects of the gap anisotropy on the tunneling spectra will also be discussed.

I. INTRODUCTION

Tunneling has been a useful tool for measuring the quasiparticle density of states and the energy gap of various superconductors since its first application to aluminum in 1962.[1] Since then, the technique has been utilized to study gap anisotropy by growing sandwich-type junctions on different faces of single crystals of elemental superconductors like Al,[2] Ga,[3] Pb,[4,5] and Sn.[6,7] These studies demonstrate that gap anisotropy can be observed directly by the tunneling method, even when the angular variation of the gap value is quite small. However, there are also materials like Nb that do not exhibit gap anisotropy in tunneling measurements.[8] It is in general believed that the scattering rate has to be minimized, and hence the condition $l \gg \xi$ (where l is the mean free path and ξ is the coherence length) must be satisfied for the observation of the gap anisotropy. High-T_c superconductors provide a perfect opportunity for gap anisotropy to be observed by tunneling because of their short coherence length. Furthermore, the gap anisotropy can provide crucial information underlying the mechanism of high-T_c superconductivity.

Progress in mechanical junctions such as breakable junctions and scanning tunneling microscopy has facilitated tunneling measurements on high-T_c superconductors. Many of these tunneling studies have been performed on $Bi_2Sr_2CaCu_2O_8$, or Bi(2212), because it cleaves easily along the a-b plane, allowing clean surfaces for both tunneling microscopy and spectroscopy. Furthermore, it is more stable against oxygen deficiency problems which occur in YBCO. A large body of tunneling data on the Bi(2212) materials is thus present in the literature[9–12] and in general the consistency of the reported energy gap values is better than that of YBCO. There have also been several tunneling studies on the gap anisotropy of Bi(2212) between the c-axis and the a-b plane directions.[13–18] All studies reported positively on the dramatic difference between the densities of states observed along these two directions. Although the interpretation of the gaplike feature along the c-axis direction can be controversial, the gap value in the a-b plane directions is quite consistently measured in these studies.

One important consideration which needs to be addressed is the gap anisotropy within the a-b plane of the high-T_c superconductors. According to many theoretical models, the in-plane gap anisotropy can actually be quite large, and in some directions (nodal lines) the gap may vanish completely. We have previously demonstrated that the in-plane gap anisotropy of Bi(2212) can be measured by controlling the tunneling direction with respect to the sample.[19,20] In this work, we will present an extensive set of data obtained from a more careful and systematic study with the same technique. In particular, we have acquired tunneling spectra from more angular locations and over a larger angular range, allowing a complete mapping of the angular dependence of the order parameter (gap). In the process, we have accumulated a very sizable number of independent gap measurements, the internal consistency of which reinforces the validity of the experimental technique and the results presented in this paper.

II. TUNNELING SPECTROSCOPY

By measuring the tunneling current (I) from a superconductor through a barrier as a function of the applied bias voltage (V), the differential tunneling conductance, $G(V) = dI/dV(V)$, can be obtained. $G(V)$, referred to as the conductance curve, can be shown to be proportional to the superconducting density of states, and will have peaks outside the gap region. In general, the intrinsic energy gap of a conventional superconducting sample can be obtained by fitting $G(V)$ with the BCS density of states (treating Δ as a parameter) modified by a depairing term Γ which accounts for the limited lifetime of the quasiparticles:

$$N(S) = N(0)\,\frac{E - i\Gamma}{\sqrt{(E - i\Gamma)^2 - \Delta^2}}. \tag{1}$$

By performing such an analysis on high-T_c tunneling data, the fitted energy gap values are significantly smaller than the values determined by the peak positions. The fitting method is in accord with the one used by photoemission measurements and the energy gap values so obtained are often close to those measured by photoemission experiments.[21,22] In the case of high-T_c tunneling, however, the quality of the fitting itself is rarely satisfactory. The major cause of difficulty in fitting the data is the presence of extra states within the gap region, as shown in Fig. 1. We have also noticed that the fits appear better only if the tunneling conductance curve is highly smeared, in which case Γ is so large that nearly all features in the spectra lose their significance.

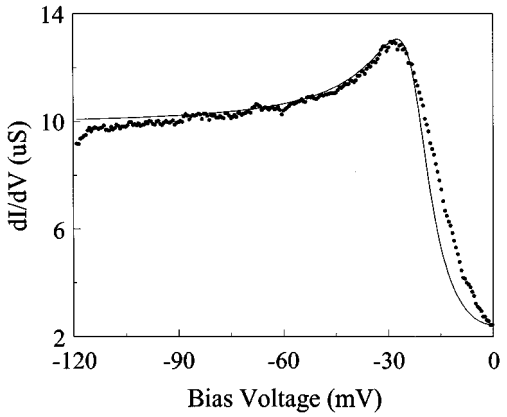

FIG. 1. A best fit (solid line) using BCS density of states and Gaussian smearing ($\Gamma=7$ meV, $\Delta=23$ meV). Note extra states within the gap region in the data.

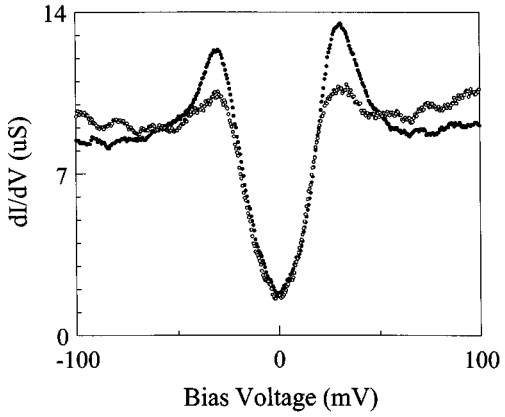

FIG. 2. Two conductance curves from the same tunneling angle. Both curves have approximately the same peak-to-peak gap value despite the difference in sharpness.

As we will discuss later in this article, the tunneling conductance curves of Bi(2212) can be fit well by assuming an angular dependence of the gap. It is our opinion that the exact form of the angular dependence is not crucial to the success of the model. Rather, the success of the model depends on having the correct symmetry in the angular dependence of the gap, along with the ability to mix in tunneling currents from angles slightly away from perpendicular to the junction. This type of model can successfully fit the high-T_c tunneling data, but the intrinsic gap cannot be described with a single value. The gap observed in the tunneling data is actually due to an integration of different intrinsic gaps over a finite angular range, and so the energy gap in the conventional sense has to be redefined. Experimentally, the simplest definition is to take the energy gap to be equal to the peak-to-peak separation divided by two for high-T_c to normal-metal (HIN) junctions, and divided by four for high-T_c to high-T_c (HIH) junctions.

There are various experimental factors that can influence the observed tunneling spectra and affect the gap value reported. For example, it has been reported that the gap value depends on surface homogeneity,[23] surface topography,[24] and also tip distance from the sample.[25] Another source of uncertainty comes from smearing due to depairing. As in the case of conventional superconductor tunneling, this smearing will increase the peak-to-peak separation and must be accounted for by fitting the conductance curves to determine the gap. Conversely, off-axis contributions to the tunneling current for highly anisotropic materials like Bi(2212) can also reduce the sharpness of the conductance curves, but will not dramatically affect the peak positions. The importance of gap anisotropy in tunneling data is nicely demonstrated in Fig. 2, where the peaks of tunneling curves of different quality taken in the same direction occur at roughly the same position. This also serves to validate the use of peak positions to determine the energy gap.

III. EXPERIMENTAL DETAILS

The in-plane tunneling spectra shown in this article were all taken using a low-temperature STM with ambient temperatures during data acquisition slightly above 4.2 K (due to heating from electronics). In order to tunnel into the a-b plane, an unconventional junction geometry was used. The edge of a thin single crystal is brought into close proximity to either a normal-metal counterelectrode (HIN junction) or the matching edge of the same crystal (HIH junction), forming a crossing configuration. For the HIN data presented in this paper, the normal-metal counterelectrode was made from a length of Pt-Ir wire. The geometry of the junctions is depicted schematically in Fig. 3. There are three important benefits which are gained from the use of this cross-junction geometry. One difference between this type of junction and a typical STM junction is the effective tunneling area. Normally, the STM tunneling area is very small and the sampling area is highly localized. The energy gap measured is therefore only a local value that depends on the stoichiometry at that position. Because a larger area of material is involved in the transport of current in the cross junctions, uncertainties due to local inhomogeneities are less significant. The second benefit is that the tunneling current is confined to the a-b plane. Earlier results show that the tunneling conductance curves taken in c-axis and a-b plane directions are qualitatively different.[15] Unless the surface is extremely well prepared, as in some other studies,[26,27] the peak features in c-axis tunneling are severely smeared and obscured by a

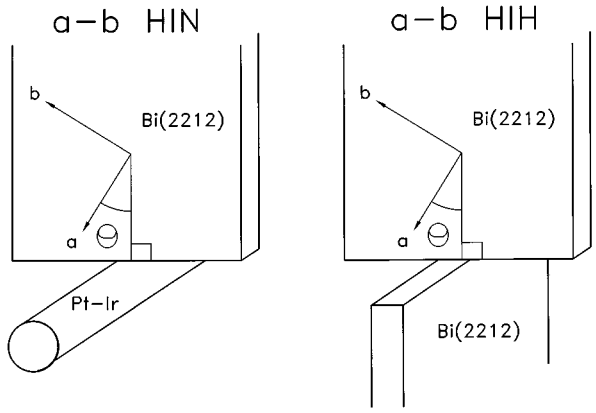

FIG. 3. Schematics of HIN and HIH junctions. θ represents the angle between the a axis (with respect to the orthorhombic unit cell) and the tunneling direction.

rising V-shaped background. It is in general believed that the V-shaped background originates from inelastic tunneling, and this view is consistent with a short c-axis coherence length. In a-b plane tunneling, however, the energy gap peaks are more prominent due to the longer coherence length in this direction. As a result, a-b plane tunneling allows a more meaningful measurement of the intrinsic gap. All tunneling curves we present in this work are consistent with the appearance of in-plane tunneling curves. The third benefit gained from this junction geometry is the capability to expose an edge perpendicular to any desired tunneling direction within the a-b plane, thereby allowing measurements of the in-plane gap in different directions. Exploitation of this tunneling technique has produced the first systematic investigation of the anisotropy of in-plane tunneling spectra of a high-T_c material to date,[20] and promises an opportunity to provide a clearer picture of the nature of high-T_c superconductivity.

The superconducting samples used in this set of experiments were carefully selected single crystal platelets (approximately $2\times2\times0.1$ mm) cleaved perpendicularly to the c axis from Bi(2212) grown by methods reported by Mitzi *et al.*[28] Four-point contact resistivity measurements showed the superconducting transition temperature to be 85 K with a transition width of 5 K. X-ray diffraction was used to ensure individual sample quality and to determine the crystallographic axes within the sample. The a and b axes are defined such that they lie within the Cu-O_2 planes, with the c axis in the perpendicular direction. In this paper, we will refer to the orthorhombic unit cell with lattice parameters of $5.414\times5.418\times30.89$ Å, in which the Cu-O_2 bond lies 45° between the a and b axes.[29] With the a and b axes known, the samples were mechanically cut to expose edges perpendicular to the desired tunneling direction and immediately transferred to the low-temperature vacuum environment. The edges were inspected with optical as well as electron microscopes, and were found to have the layered structure of the bulk material still intact and unaltered by the cutting process. Figure 4 shows a scanning electron micrograph of a typical edge cut using the mechanical process. The layered structure is clearly intact in this and all other micrographs we have taken. The layers apparent in this micrograph are approximately 2.0 μm across, which translates to roughly 650 unit cells in the c-axis direction. Once the sample is locked into position with its edge perpendicular to the counterelectrode, the two are carefully brought into close proximity until a tunneling current is detected. The tunneling current as a function of applied bias voltage is then measured, and the differential conductance is derived from the data. For a each sample, several edges with different crystallographic orientations are cut and characterized. Many series of spectra are then taken from each edge by maneuvering the counterelectrode or reapproaching. Thus, a record of the in-plane tunneling spectra in various directions is collected. In order to make a mapping of the energy gap values taken from this data over a wide angular range, three different samples were used. In all cases the tunneling spectra from the different samples are comparable, and continuity of the data between samples is intact.

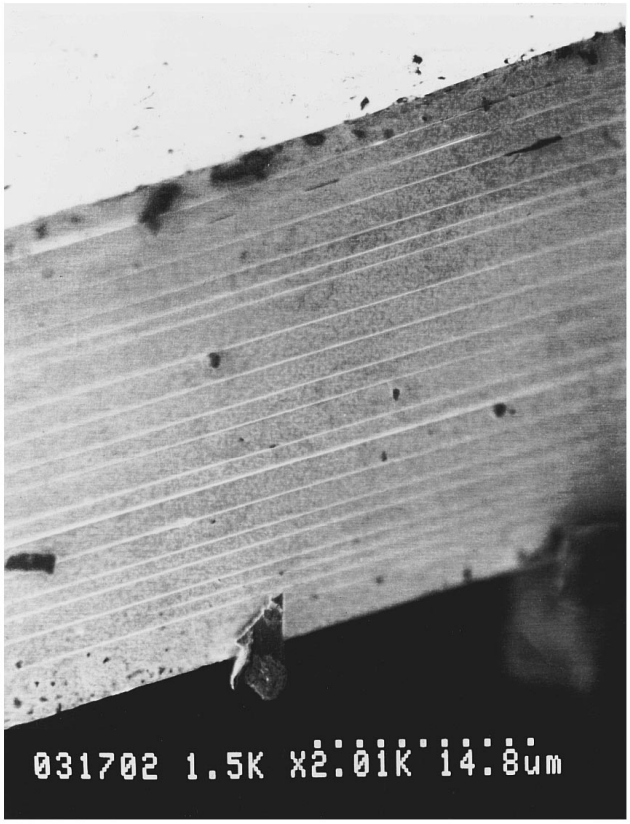

FIG. 4. Scanning electron micrograph of a typical edge cut using the mechanical process. The layered structure is preserved and the layers are approximately 2.0 μm across.

IV. RESULTS AND DISCUSSION

To demonstrate the in-plane gap anisotropy, we first compile selected data from three separate samples. In the following, all curves in the same figure are data collected in the same measurement run from the same piece of sample, and angles are measured from the a axis (with respect to the orthorhombic unit cell). In Fig. 5, we show typical tunneling conductance curves taken along four different directions ranging from 11° to 44° within the a-b plane of the sample. The peak-to-peak separation divided by two (energy gap) is 33 meV at 11°, and reaches a minimum of 18 meV at 44°, which corresponds to tunneling along the Cu-O_2 bond direction. To locate the maximum and minimum gap values with certainty, we extended the angular range of the data by performing the same experiment on two other samples. Curves taken with tunneling angles ranging from 25° to 65° are displayed in Fig. 6. The energy gap reaches a minimum of 23 meV at 45° and increases to 30 meV 20° away. The minimum of the energy gap can now be unambiguously located at 45° (Cu-O_2 bond direction). In Fig. 7, we have compiled another set of five curves with tunneling directions ranging from $-20°$ to $+20°$ with 0° in between. Here we observe that the change in the energy gap is not as dramatic near the maximum gap (0°) direction. The peak position varies only slightly in this angular range, with a gap (Δ) difference of about 5 meV. Over the entire 45° range, Δ has a variation of about 20 meV, from a maximum of 40 meV to a minimum of 20 meV.

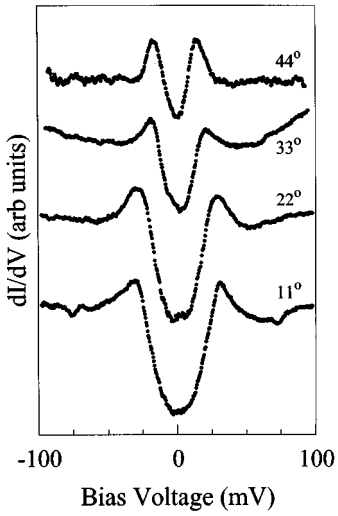

FIG. 5. Conductance curves from four angles within the same sample. The peak-to-peak gap values are strongly dependent on the tunneling angle. All curves are normalized so that the distance between the peaks and zero conductance are the same. They are then shifted upward for presentation clarity.

Although the curves taken along the gap minimum directions in Figs. 5 and 6 look as sharp or sharper than the others, we want to point out that the zero bias offset of these curves is significantly larger than those of the other curves, and that this offset is included in the normalization. As a result, the 45° curves appear to be more shallow than the other curves. Indeed, in the data we have collected so far, there is an obvious trend that the zero bias offset increases near the minimum gap direction. This suggests that normal electron tunneling plays an important role in this angular range. When inspecting the quality of tunneling conductance curves of the conventional superconductors, a large zero bias offset is often considered to indicate electrical shorting past the insulating barrier, and thus data of poor quality. In the case of highly anisotropic materials such as the high-T_c superconductors, the zero bias offset can be due to the gap anisotropy and therefore is not sufficient to determine the quality of the data.

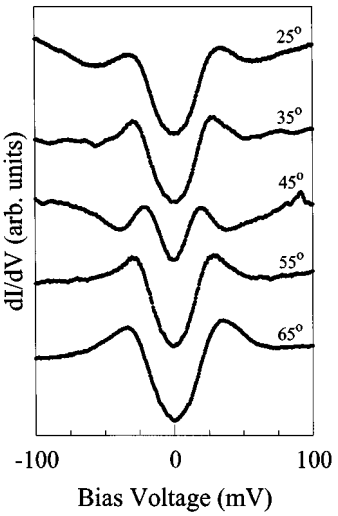

FIG. 6. Conductance curves from five angles within the same sample. The gap minimum is located with certainty at 45° (along the Cu-O_2 bond).

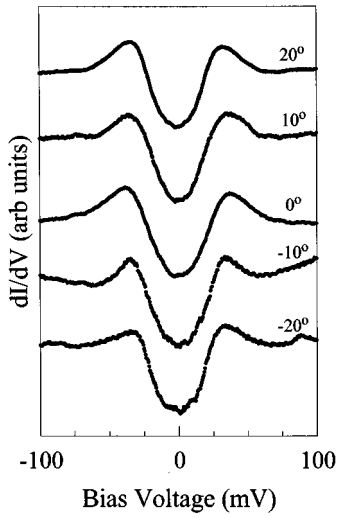

FIG. 7. Conductance curves centered about the gap maximum. The gap anisotropy is smaller in this angular region.

A comprehensive presentation of the data appears in Fig. 8, which shows the measured gap (peak-to-peak divided by 2) values derived from our HIN data verses the tunneling direction. This plot shows all of the data taken from the three different Bi(2212) single crystals represented in Figs. 5–7. The measured gap values range from 40 meV at 0° from the *a* axis to 18 meV at 45°, where 45° indicates tunneling along the Cu-O_2 bond. At each tunneling angle there is a spread in the measured gap values which remains roughly constant at about 8 meV. This spread is significantly smaller than the measured anisotropy, and can be primarily accounted for by smearing due to depairing effects. Smaller experimental errors due to uncertainty in tunneling angle and finite energy resolution can also contribute. The angular range over which the HIN gap measurements were taken span 90° of the total

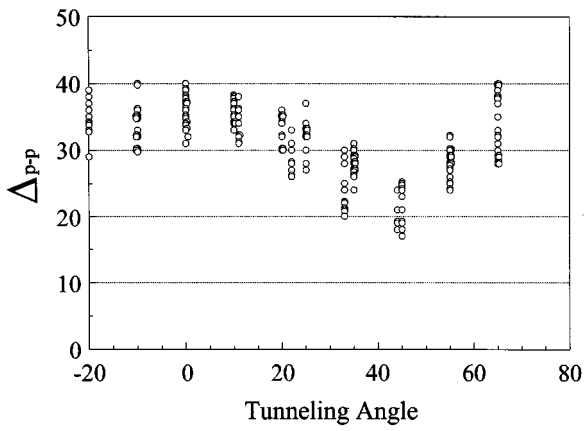

FIG. 8. Energy gap values plotted against tunneling angle from all measurements in this study. The gap reaches a pronounced minimum at 45° (Cu-O_2 bond direction) although no nodal line is detected. The uncertainty in gap measurements at a given angle is smaller than the anisotropy. The anisotropy is greatest near the gap minimum, and is quite small near the gap maximum.

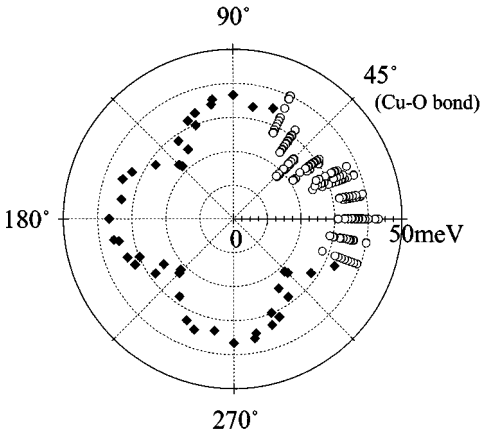

FIG. 9. By assuming a fourfold symmetry, the data in Fig. 8, which encompass 90°, can be used to map the measured gap values to 360°. The open circles are the actual data, the solid diamonds are averages of the data.

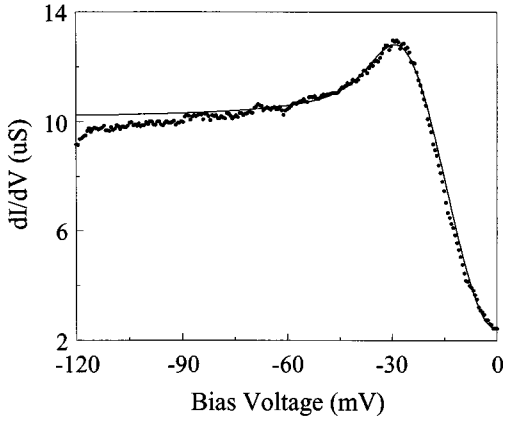

FIG. 10. By incorporating an anisotropic gap function into the fitting model, extra states within the gap region are introduced. This dramatically improves the quality of the fit (solid line) as compared to the fit in Fig. 1 of the same data.

360° of the real space a-b plane, including a gap minimum at 45° and a maximum centered about 0° with respect to the a axis. The crystal structure is orthorhombic but includes a one-dimensional in-plane superstructure along the b axis.[29] Apart from this superstructure which has not been shown to affect the electric, magnetic, or superconducting properties of the material, the system possesses a fourfold symmetry. By assuming that this fourfold symmetry can be applied to the angular dependence of the gap function, a mapping of the gap anisotropy may be extrapolated for the full 360°. Figure 9 is a polar plot which depicts the symmetry of the gap suggested by our data. The experimental data are plotted and a mean gap value calculated for each tunneling angle. These mean values are then used to map the anisotropy pattern to the remaining angular range.

An important distinction between the competing theories which describe the mechanism responsible for high-temperature superconductivity is the pairing state of the superconducting electrons. One conspicuous feature of a d-wave pairing mechanism is the existence of a nodal line in the angular dependence of the energy gap which would, in theory, manifest itself as a point where the gap would pass through zero, changing sign. Tunneling experiments are not sensitive to this sign change, but should be able to detect the rapid approach to zero. Only phase-sensitive measurements[30,31] can ensure the existence of a nodal line. It is difficult to conclude whether or not a nodal line exists purely by inspection of the data in Figs. 8 and 9. The rate of change of the measured gap values is indeed largest near the gap minimum direction (45°), while the gap values measured in the angular range near the gap maximum (0°), change more slowly. This may imply that a singularity exists in the angular dependence of the energy gap, but no direct evidence of a nodal line has been observed in this experiment. Two explanations for the failure to detect the nodal line may be advanced. It is possible that the nodal line does not exist at all. The angular dependence of the gap we observe may be described consistently by models with anisotropic s-wave components.[32] Conversely, limits in the angular resolution of the tunneling experiment may prohibit the resolution of the nodal line. These limits have their origin in the fact that tunneling currents from directions away from perpendicular to the junction contribute to the overall current density, although with a magnitude which falls off exponentially with increasing angle from perpendicular. This effect can mask a zero gap measurement along a nodal line by sampling currents from nearby angular ranges.

Although we make no claims as to whether a nodal line exists or not, it should be noted that excellent fits of data taken with this technique on Bi(2212) have been generated previously by assuming a d-wave dependence of the energy gap.[20] To demonstrate this explicitly, we apply the same fitting procedure to a typical curve from our present data, shown in Fig. 10. In this fitting, we have assumed a d-wave-like gap anisotropy with a nodal line along the Cu-O_2 bond direction. However, in a particular direction, we still assume the BCS density of states as given in Eq. (1) with $\Gamma=0$. To obtain the tunneling conductance curve, we allow tunneling in other directions with an exponential weight $\exp(-\beta \sin^2\theta)$, where β is a parameter which depends on the work function and the barrier thickness. For high-T_c superconductors, the work function and β are in general smaller than many other metals.[33] This reduces the angular resolution of the present measurement. On rare occasions, most likely due to surface conditions, β can be larger and tunneling is limited to a smaller angular range. This may explain why BCS-like conductance curves with relatively sharp peaks and small zero bias offset are observed in some other tunneling experiments. Depairing effects are taken into account by smearing each data point with a Gaussian function of Γ in width. As can be seen by comparing Figs. 1 and 10, the inclusion of gap anisotropy has effectively produced extra states within the gap region and improved the quality of fitting dramatically. The importance of this exercise is that, though the nodal line is not observed, there is no contradiction between our data and the existence of a nodal line if the limited angular resolution is taken into account. This procedure works well for all of our data, and a similar approach has also been successfully applied by other researchers to analyze angular resolved tunneling spectra.[34]

Another distinction between theories of the high-T_c pairing mechanism is the orientation of the gap function. This is

a question which the present result could help to answer. Although many of the models which predict gap anisotropy are ambivalent to the orientation of the gap function with respect to the crystallographic axes, some models do predict a specific orientation. For example, Pines *et al.*[35] have proposed an interaction between planar quasiparticles induced by the exchange of antiferromagnetic paramagnons, and have demonstrated that this model leads uniquely to a superconducting state with $d(x^2-y^2)$ symmetry. This form for the gap symmetry would identify the Cu-O_2 bond direction with the gap maximum. It should be pointed out, however, that the dispersion relation obeyed by the planar quasiparticles was determined by angular-resolved photoemission (ARPES) experiments, and that the spectrum of spin fluctuations was taken from fits to NMR experiments.[36] Conversely, Miyake *et al.*[37] have calculated the interaction for spin-singlet Cooper pairs and conclude that the interaction is attractive for the $d(xy)$ symmetry, but repulsive for both extended-s and $d(x^2-y^2)$ symmetries. The $d(xy)$ symmetry would place the gap minimum along the Cu-O_2 bond direction. Depending on the filling of the Fermi surface, Anderson's anisotropic s-wave model, in which the underlying mechanism is an interlayer tunneling phenomenon, could also identify the Cu-O_2 bond as the gap minimum.[38]

One important difference between the results of the present experiment and those of recent ARPES experiments involves this orientation of the gap function. The present experiment identifies the Cu-O_2 bond direction as the energy gap minimum, while the photoemission results identify it as the gap maximum. In other words, the photoemission gap anisotropy pattern is rotated by 45° from our results. While agreement on the direction of the maximum (or minimum) energy gap from independent photoemission groups has been demonstrated,[39–41] our results have also been reproduced by other researchers.[42] Furthermore, Tanaka *et al.* have extended tunneling measurements to the materials $YBa_2Cu_3O_7$ and $La_{2-x}Sr_xCuO_4$ ($x=0.10$ and 0.15) and obtained similar results with the minimum gap along the Cu-O bond direction.[42] Hence, it seems certain that there is a systematic difference between tunneling and photoemission measurements. Ueda *et al.*[43] has proposed the possibility that the current measured by tunneling is actually 45° off from the normal to the surface by considering the shape of the electron wave function of the surface oxygen. They argue that the tunneling probability depends on the orientation of the oxygen orbitals. For example, when a measurement is taken along the minimum gap direction, the orbitals can be 45° off the surface and the tunneling electrons would be more likely to come from the maximum gap direction. Miyake *et al.*,[44] on the other hand, has recently made a similar comment on photoemission results. He contends that the photoemission intensity is actually weaker when the energy gap is maximum because the coherence factor is small at $\hbar\omega>2\Delta$ for a type-II process. None of these authors demonstrate how the angular change of photoemission intensity or tunneling current strength will affect the peak position observed and the gap value measured. It is therefore important that more careful analysis and further experiments be pursued to resolve the difference.

In order to demonstrate the validity of our HIN tunneling data, we have also performed in-plane Bi(2212) to Bi(2212)

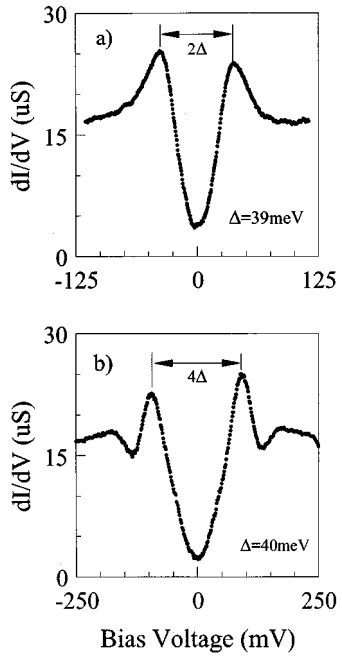

FIG. 11. Conductance curves taken from (a) HIN tunneling and (b) HIH tunneling. The measured gap values are approximately the same (note that the bias voltage scales are different). Both curves were taken along the 0° (gap maximum) direction.

(HIH) tunneling using a similar junction structure. In particular, we will show the consistency in the data taken from the two different techniques, and provide additional evidence of the measured gap anisotropy. As in the HIN experiments, x-ray diffraction was used to determine the crystallographic axes within the sample, and the sample was dissected to expose an edge with either the 45° or 0° direction perpendicular on both halves (see Fig. 3). The samples were then immediately transferred to the STM. For simplicity of analysis in these HIH experiments, measurements were made only at a single angle for each sample and hence the tunneling angles at both sides are the same. In Fig. 11 we compare two conductance curves taken at 0° using HIN and HIH tunneling. As we have reported before,[15] the semiconductor model commonly used for HIN tunneling can also be applied to HIH tunneling. According to this model, the peak-to peak separation in HIH data (4Δ) should be twice that of HIN data (2Δ), and the data shown in Fig. 11 conform well to this expectation. Although the HIH and HIN curves are consistent in peak positions, it is clear that there are also some striking differences in the shapes of these curves. The conductance peaks are much sharper and more pronounced in the HIH data, as is to be expected from the simplest models of superconducting tunnel junctions. There is also an interesting dip feature, reported previously by other researchers,[45] which is obscured in the HIN data but can be clearly seen in the typical HIH spectrum. Explanations for this feature have been proposed in theoretical models.[46,47] We observe this dip feature clearly in both the maximum and minimum gap directions, in contrast to some earlier photoemission reports.[21] In the experiment above, the majority of the tunneling spectra showed this dip feature clearly, and it appeared with equal frequency in the 0° and 45° directions.

To examine the gap anisotropy, samples with edges cut in

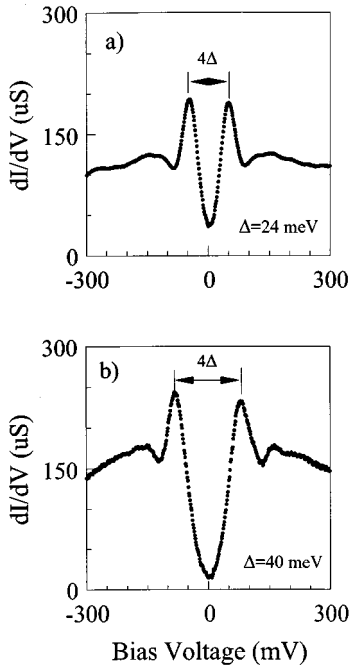

FIG. 12. Conductance curves from HIH tunneling along the directions (a) 45°, and (b) 0°. The gap measurements are consistent with those from HIN data in magnitude and angular dependence. As with HIN tunneling, the zero bias offset is larger in the small gap direction.

different directions were used. Figure 12 shows two typical HIH tunneling conductance curves from these measurements, taken along the expected minimum and maximum gap directions. The measured gap values at 0° and 45° are 40 meV and 23 meV, respectively. This is in complete agreement with results from the HIN measurements, although it should be pointed out that there is a spread in measured gap values in the HIH tunneling data, as in the HIN case. This can be seen in Fig. 13, which provides a plot of all of the energy gap values taken from HIH tunneling in the two different directions. The uncertainty in the measured gap values is approximately the same in both HIH and HIN tunneling, even though the HIH spectra is sharper. Most importantly, the measured gap values are clearly smaller in the 45° direction (along the Cu-O_2 bond) than in the 0° direction, in agreement with the angular dependence established from the HIN data.

V. CONCLUSIONS

We have measured the in-plane energy gap of Bi(2212) at 14 different angular locations within a 90° range. The angular dependence of the energy gap is completely mapped out

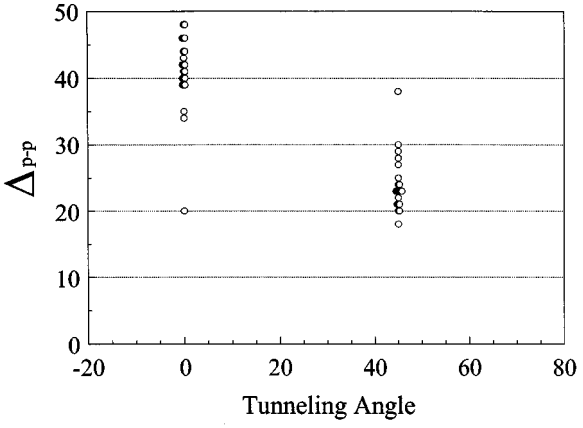

FIG. 13. A plot showing all measured gap values from HIH junctions. The gap anisotropy pattern is the same as from HIN junctions, but the uncertainty is not improved.

by assuming a fourfold symmetry as holds approximately in the crystal structure. The in-plane gap anisotropy is clearly observed with a minimum value of 20 meV along the Cu-O_2 bond. The maximum gap direction is 45° away, with a value of about 40 meV. The anisotropy pattern as well as the gap values were confirmed by high-T_c to high-T_c tunneling. It is not clear why there is a 45° difference between tunneling and photoemission results, though different explanations have been proposed by other researchers.

At a specific angle, there is an experimental uncertainty of about 8 meV in the measured energy gap values due to depairing effects and other experimental factors. This uncertainty is approximately the same along all tunneling directions, and more importantly, it is significantly smaller than the gap variation due to anisotropy. The gap value varies most rapidly near the minimum gap direction. We observe no direct evidence of a nodal line in the angular dependence of the gap, however we cannot ignore the possibility of a nodal line due to limitations in angular resolution.

ACKNOWLEDGMENTS

All samples used in the HIN experiments are high-quality Bi(2212) single crystals provided by Farun Lu and Professor E. L. Wolf of the Polytechnic University, New York. Samples used in the HIH experiments were grown by our colleague Tim Symons. We would like to thank Professor C. P. Brock of the Chemistry Department at the University of Kentucky for her assistance and advice concerning x-ray diffraction work. We also wish to thank Professor Robert J. Jacob of U. K.'s Department of Microbiology and Immunology for the electron micrographs of the Bi(2212) edge. This work was supported by the National Science Foundation through Grant No. DMR-9307328.

[1] I. Giaever and H. R. Zeller, Phys. Rev. Lett. **20**, 1504 (1968).
[2] B. L. Blackford, J. Low. Temp. Phys. **23**, 43 (1976).
[3] V. R. Kalvey and W. D. Gregory, Phys. Lett. **74A**, 256 (1979).
[4] B. L. Blackford and R. H. March, Phys. Rev. **186**, 397 (1969).
[5] G. I. Lykken, A. L. Geiger, K. S. Dy, and E. N. Mitchell, Phys. Rev. B **4**, 1523 (1971).
[6] N. V. Zavaritskii, Sov. Phys. JETP **48**, 837 (1965).
[7] B. L. Blackford and K. Hill, J. Low Temp. Phys. **43**, 25 (1981).

[8] J. Bostock, K. Agyeman, M. H. Frommer, and M. L. A. MacVicar, J. Appl. Phys. **44**, 5567 (1973).
[9] T. Ekino and J. Akimitsu, Phys. Rev. B **40**, 6902 (1989).
[10] H. J. Tao, A. Chang, Farun Lu, and E. L. Wolf, Phys. Rev. B **45**, 10 622 (1992).
[11] Zhe Zhanf and Charles M. Lieber, J. Phys. Chem. **96**, 2030 (1992).
[12] K. Kitazawa and T. Hasegawa, in *Physical Properties of High T_c Superconductors*, edited by D. M. Ginsberg (World Scientific, Singapore, 1992), Vol. 3, pp. 525–622.
[13] G. Briceno and A. Zettl, Solid State Commun. **70**, 1055 (1989).
[14] M. F. Crommie, G. Briceno, and A. Zettl, Physica C **162-164**, 1397 (1989).
[15] Qun Chen and K.-W. Ng, Phys. Rev. B **45**, 2569 (1992).
[16] M. Boekholt, M. Hoffmann, G. Gunthrodt, Physica C **175**, 127 (1991).
[17] Koichi Ichimura and Kazushige Nomura, J. Phys. Soc. Jpn. **62**, 3661 (1993).
[18] D. Mandrus, L. Forro, D. Koller, and L. M. Mihaly, Nature (London) **351**, 460 (1991).
[19] J. Kane, Qun Chen, and K.-W. Ng, Physica B **194-196**, 1735 (1994).
[20] Jeffrey Kane, Qun Chen, K.-W. Ng, and H.-J. Tao, Phys. Rev. Lett. **72**, 128 (1994).
[21] D. S. Dessau, B. O. Wells, Z.-X. Shen, W. E. Spicer, A. J. Arko, R. S. List, D. B. Mitzi, and A. Kapitulnik, Phys. Rev. Lett. **66**, 2160 (1991).
[22] Y. Hwu, L. Lozzi, M. Marsi, S. La Rosa, M. Winokur, P. Davis, and M. Onellion, Phys. Rev. Lett. **67**, 2573 (1991).
[23] E. L. Wolf, A. Chang, Z. Y. Rong, Yu. M. Ivanchenko, and Farun Lu, J. Supercond. **7**, 355 (1994).
[24] Jin-Xiang Liu, Ji-Chun Wan, A. M. Goldman, Y. C. Chang, and P. Z. Jiang, Phys. Rev. Lett. **67**, 2195 (1991).
[25] Tetsuya Hasegawa, Masashi Nantoh, and Koichi Kitazawa, Jpn. J. Appl. Phys. **30**, L276 (1991).
[26] Ch. Renner and Ø. Fischer, Physica C **235-240**, 53 (1994).
[27] H. L. Edwards, J. T. Markert, and A. L. deLozanne, Phys. Rev. Lett. **69**, 2967 (1992).
[28] D. M. Mitzi, L. W. Lombardo, A. Kapitulnik, S. S. Ladermann, and R. D. Jacowitz, Phys. Rev. B **41**, 6564 (1990).
[29] S. A. Sunshine, T. Siegrist, L. F. Schneemeyer, D. W. Murphy, R. J. Cava, B. Batlogg, R. B. van Dover, R. M. Fleming, S. H. Glarum, S. Nakahara, R. Farrow, J. J. Krajewski, S. M. Zahurak, J. V. Waszczak, J. H. Marshall, P. Marsh, L. W. Rupp, Jr., and W. F. Peck, Phys. Rev. B **38**, 893 (1988).
[30] J. R. Kirtley, C. C. Tsuei, J. Z. Sun, C. C. Chi, Lock See Yu-Jahnes, A. Gupta, M. Rupp, and M. B. Ketchen, Nature **373**, 225 (1995).
[31] D. A. Wollman, D. J. Van Harlingen, J. Giapintzakis, and D. M. Ginsberg, Phys. Rev. Lett. **74**, 797 (1995).
[32] G. D. Mahan, Phys. Rev. B **48**, 16557 (1993). See also G. D. Mahan, Phys. Rev. Lett. **71**, 4277 (1993).
[33] Chen Wang, B. Giambattista, C. G. Slough, R. V. Coleman, and M. A. Subramanian, Phys. Rev. B **42**, 8890 (1990).
[34] Shukichi Tanaka, Eiji Ueda, and Masatoshi Sato, Physica C **224**, 126 (1994).
[35] P. Monthoux, A. V. Balatsky, and D. Pines, Phys. Rev. B **46**, 14803 (1992).
[36] P. Monthoux and D. Pines, Phys. Rev. B **49**, 4261 (1994).
[37] T. Tsuji, O. Narikiyo, and K. Miyake, Physica C **226**, 333 (1994).
[38] Sudip Chakravarty, Asle Sudbø, Philip W. Anderson, and Steven Strong, Science **261**, 337 (1993).
[39] R. J. Kelly, Jian Ma, G. Margaritondo, and M. Onellion, Phys. Rev. Lett. **71**, 4051 (1993).
[40] Z.-X. Shen, W. E. Spicer, D. M. King, D. S. Dessau, and B. O. Wells, Science **27**, 267 (1995).
[41] H. Ding, J. C. Campuzano, A. F. Bellman, T. Yokoya, M. R. Norman, M. Randeria, T. Takahashi, H. Katayama-Yoshida, T. Mochiku, K. Kadowaki, and G. Jennings, Phys. Rev. B **74**, 2784 (1995).
[42] Shukichi Tanaka, Eiji Ueda, Masatoshi Sato, Kenji Tamasaku, and Sin-ichi Uchida, J. Phys. Soc. Jpn. Lett. **64**, 1476 (1995).
[43] Eiji Ueda, Shukichi Tanaka, Masatoshi Sato, Kenji Tamasaku, and Sin-ichi Uchida, Physica C **249**, 181 (1995).
[44] Kazumasa Miyake and Osamu Narikiyo, J. Phys. Soc. Jpn **64**, 1040 (1995).
[45] J. F. Zasadzinski, N. Tralshawala, P. Romano, Q. Huang, Jun Chen, and K. E. Grey, J. Phys. Chem. Solids **53**, 1635 (1992).
[46] S. H. Liu and R. A. Klemm, Phys. Rev. B **48**, 10 650 (1993).
[47] D. Coffey and L. Coffey, Phys. Rev. Lett. **70**, 1529 (1993).